university of groningen

University Medical Center Groningen

University of Groningen

# A dearth of dark matter in strong gravitational lenses

Sanders, R. H.

*Published in:*
Monthly Notices of the Royal Astronomical Society

*DOI:*
10.1093/mnras/stu057

**IMPORTANT NOTE: You are advised to consult the publisher's version (publisher's PDF) if you wish to cite from it. Please check the document version below.**

*Document Version*
Publisher's PDF, also known as Version of record

*Publication date:*
2014

Link to publication in University of Groningen/UMCG research database

*Citation for published version (APA):*
Sanders, R. H. (2014). A dearth of dark matter in strong gravitational lenses. *Monthly Notices of the Royal Astronomical Society*, *439*, 1781-1786. https://doi.org/10.1093/mnras/stu057

**Copyright**
Other than for strictly personal use, it is not permitted to download or to forward/distribute the text or part of it without the consent of the author(s) and/or copyright holder(s), unless the work is under an open content license (like Creative Commons).

The publication may also be distributed here under the terms of Article 25fa of the Dutch Copyright Act, indicated by the “Taverne” license. More information can be found on the University of Groningen website: https://www.rug.nl/library/open-access/self-archiving-pure/taverne-amendment.

**Take-down policy**
If you believe that this document breaches copyright please contact us providing details, and we will remove access to the work immediately and investigate your claim.

*Downloaded from the University of Groningen/UMCG research database (Pure): http://www.rug.nl/research/portal. For technical reasons the number of authors shown on this cover page is limited to 10 maximum.*

Download date: 05-05-2023

Monthly Notices
of the
ROYAL ASTRONOMICAL SOCIETY

MNRAS **439,** 1781–1786 (2014)
Advance Access publication 2014 February 10

doi:10.1093/mnras/stu057

# A dearth of dark matter in strong gravitational lenses

R. H. Sanders★

*Kapteyn Astronomical Institute, PO Box 800, NL-9700 AV Groningen, the Netherlands*

Accepted 2014 January 8. Received 2013 December 27; in original form 2013 October 23

**ABSTRACT**

I show that the lensing masses of the Sloan Lens Advanced Camera Surveys sample of strong gravitational lenses are consistent with the stellar masses determined from population synthesis models using the Salpeter initial mass function. This is true in the context of both General Relativity and modified Newtonian dynamics (MOND), and is in agreement with the expectation of MOND that there should be little classical discrepancy within the high surface brightness regions probed by strong gravitational lensing. There is also dynamical evidence from this sample supporting the claim that the mass-to-light ratio of the stellar component increases with the velocity dispersion.

**Key words:** gravitational lensing: strong – galaxies: elliptical and lenticular, cD – galaxies: haloes – dark matter.

## 1 INTRODUCTION: MASS DISCREPANCIES IN ELLIPTICAL GALAXIES

Modified Newtonian dynamics, MOND (Milgrom 1983), is a non-relativistic theory that posits the existence of a critical acceleration ($a_0 \approx 10^{-8}$ cm s$^{-2}$) below which the effective gravitational acceleration $g$ deviates from Newtonian form ($g_{\rm N}$) in a specific way – in effect, $g \rightarrow \sqrt{a_0 g_{\rm N}}$ when $g < a_0$. The motivation is to remove the need for dark matter in gravitationally bound astronomical systems with low internal and external accelerations ($g < a_0$). The critical acceleration can also be expressed as a surface density ($\approx a_0/G$), the implication being that discrepancies between the classical dynamical mass and the observable baryonic mass should appear in low surface density, or low surface brightness, systems. Conversely, there should be no significant discrepancy within high surface brightness systems.

Rotation curves of the neutral gas in disc galaxies as measured in the 21 cm line present obvious advantages in tracing the gravitational acceleration as a test of MOND: cool gas, generally in planar circular motion, provides an unambiguous tracer of the acceleration and deviations from such motions can usually (but not always) be identified; moreover, random motions are small and generally do not contribute to the support of the gas disc against gravity (Trachternach et al. 2008).

The success of MOND when confronted by the extensive body of data on measured rotation curves, ranging from gas-rich low surface brightness dwarfs (Swaters, Sanders & McGaugh 2010) to high surface brightness earlier type disc galaxies dominated by a stellar component (Sanders & Noordermeer 2007), can hardly be disputed. This success plus the observed and theoretically predicted baryonic Tully–Fisher relation (McGaugh 2005) constitute the principal evidence supporting MOND. However, gas-poor early-type systems, ellipticals and S0s, usually miss such a clear tracer of the gravitational acceleration; for such objects the situation has been more confused.

An unavoidable prediction of MOND is that in high surface brightness systems, such as luminous elliptical galaxies, there should be little discrepancy between the detectable baryonic mass and the Newtonian dynamical mass within the bright luminous object. In other words, with the traditional Newtonian analysis, there should be no evidence for dark matter within the projected radius containing half the flux of visible light, the effective radius. This, in fact, was the result of the observational study of Romanowsky et al. (2003). They used the observed kinematics of bright planetary nebulae as a tracer of the mass distribution in three nearby elliptical galaxies, and found that the results were consistent with no substantial dark matter contribution within four effective radii, a result shown by Milgrom & Sanders (2003) to be in agreement with the expectations of MOND.

The use of such stellar tracers suffers from the ambiguity introduced by the uncertain distribution of stellar orbits, but Milgrom (2012) has recently demonstrated that the pressure distribution of the hot X-ray emitting gaseous envelopes in two isolated elliptical galaxies, extending out to 100 kpc and over a range of a factor of 100 in acceleration, is entirely consistent with the run of gravitational accelerations calculated from the observed distribution of visible stars using the MOND algorithm. The implied mass-to-light ratios ($M/L$s) of the stellar populations are sensible for early-type galaxies. Subsequently, Milgrom (2013) pointed out that the statistics of galaxy–galaxy weak gravitational lensing (the small distortions in the shapes of background galaxies in the field of nearer foreground galaxies), which probes accelerations down to a few per cent of $a_0$, implies that the asymptotic velocity dispersion of fitted isothermal spheres is related to the baryonic mass of the deflecting galaxies as $M \propto \sigma^4$, exactly as required by MOND – an elliptical galaxy

★ E-mail: sanders@astro.rug.nl

© 2014 The Author
Published by Oxford University Press on behalf of the Royal Astronomical Society

Downloaded from https://academic.oup.com/mnras/article-abstract/439/2/1781/1013236 by University of Groningen user on 16 November 2018

equivalent to the baryonic Tully–Fisher relation in spiral galaxies. In other words, it appears that the dynamics of the outer 'haloes', more than 100 kpc in extent, is determined by the small fraction of baryons in the very centre, a very strange fact indeed when viewed in the context of dark matter.

On the other hand, there are persistent claims that strong gravitational lensing, the formation of multiple images or Einstein rings of background sources by foreground galaxies, require the presence of substantial quantity of dark matter within one or two effective radii in early-type galaxies. If true, this would appear to be in contradiction to the predictions of MOND because strong lensing can only occur in the high-acceleration regime (see the discussion below). There has been controversy about this issue in the literature, with some authors claiming that no dark matter is required (Chen & Zhao 2006; Chiu, Ko & Tian 2006; Sanders & Land 2008; Chiu et al. 2011), while others argue that strong lensing requires that substantial fraction of the total mass (up to 80 per cent) is dark within two effective radii (Ferreras et al. 2009, 2012; Mavromatos, Sakellariadou & Yusaf 2009; Leier et al. 2011).

This problem is complicated by the possibility of contamination – whether or not distant lenses are truly isolated or lying within groups or clusters – and by the uncertainty of the $M/L$ of the underlying stellar population. With respect to this second problem – that of the stellar $M/L$ – there is recent evidence, spectroscopic and dynamical, that the initial mass function (IMF) of stars formed in early-type galaxies is not universal, as is often supposed, but becomes increasingly bottom heavy – weighted towards lower mass stars – in higher mass galaxies. That is to say, the IMF is better described by that of Salpeter (1955) rather than that of Chabrier (2003) in systems with higher velocity dispersion or total mass. This in turn implies that the total stellar $M/L$ is higher in more massive galaxies (there is about a factor of 2 difference in $M/L$ between model populations constructed with the Chabrier versus Salpeter IMFs).

Spectroscopic evidence for an increasingly dominant contribution of dwarf stars has been given by Conroy & van Dokkum (2012), Smith, Lucey & Carter (2012) and Spiniello et al. (2012, 2013). Conroy et al. (2013) have provided dynamical evidence that in compact elliptical galaxies (in which dark matter presumably does not dominate), the stellar $M/L$ increases systematically with galaxy velocity dispersion. The evidence of Spiniello et al. (2013), using spectroscopic tracers of low-mass stars, similarly suggests an almost linear increase in the stellar $M/L$ with velocity dispersion.

Here, in view of these developments, I reconsider the question of whether or not the MOND lensing masses of strong lens systems are consistent with the stellar masses in the Sloan Lens Advanced Camera Surveys (SLACS) sample of gravitational lenses.

## 2 A COMMENT ON STRONG LENSING WITH MOND

Unlike General Relativity (GR), MOND is a non-relativistic theory. That means that MOND in itself says nothing about gravitational lensing and other relativistic effects. There have now been several proposed candidate relativistic extensions of MOND (see Famaey & McGaugh 2012 for a recent review) but there is no generally accepted theory. In most of these proposals, the relationship between the deflection of photons and the weak field force, also in the low-acceleration limit, is required to be the same as it is in GR. This is built into the theories and, in fact, required by apparent coincidence of the classical dynamical mass of clusters of galaxies (using galaxy kinematics or the distribution of hot gas – non-relativistic particles) and the lensing mass of the clusters (the effect of gravity on photons – relativistic particles). Therefore, it is not yet particularly meaningful to apply a specific relativistic theory, such as the Tensor-Vector-Scalar theory (TeVeS; Bekenstein 2004), to the problem of lensing; the suggested interpolating functions are just as arbitrary as those typically used in MOND. So here I will use one of the usual MOND interpolating functions that works well for galaxy rotation curves, the so-called simple form recommended by Zhao & Famaey (2006), i.e.

$$\mu(x) = x/(1+x) \tag{1}$$

with $x = g/a_0$.

The MOND algorithm is given by

$$g\mu(g/a_0) = g_{\rm N}, \tag{2}$$

where I take $a_0 = 10^{-8}$ cm s$^{-2}$. Viewing MOND as a modification of gravity, this formula is only strictly true in spherical systems.

It can be shown that, with GR, for a spherically symmetric gravitational lens, perfectly aligned with a small background source, an Einstein ring will be formed if the enclosed mean surface density in the lens exceeds

$$\Sigma_{\rm crit} = \frac{cH_0}{4\pi G} F(z_{\rm l}, z_{\rm s}), \tag{3}$$

where $F(z_{\rm l}, z_{\rm s})$ is a dimensionless function of the lens and source redshifts (related to the angular size distances in units of the Hubble distance, $c/H_0$); for the lenses considered here $F \approx 10$.

The critical surface density below which MOND phenomenology appears is roughly

$$\Sigma_{\rm M} \approx a_0/\pi G. \tag{4}$$

Given that $a_0 \approx cH_0/6$ we find that, typically,

$$\Sigma_{\rm crit} \approx (\pi/2)\Sigma_{\rm M} F(z_1, z_2) \approx 15\Sigma_{\rm M}. \tag{5}$$

Therefore, strong lensing always occurs in the high-acceleration limit. No large discrepancy should be detected by strong gravitational lensing (the minimum value of $F$ in a concordance cosmology is 3.4, so it is always the case that $\Sigma_{\rm crit} > \Sigma_{\rm M}$).

That is not to say that no discrepancy whatsoever should be present within an Einstein ring radius. MOND can be represented by a halo of phantom dark matter – the dark matter that one would presume to be present if the MOND phenomenology were to be represented by a dark halo. The space density of phantom dark matter is given by

$$\rho_{\rm pdm} = -\frac{1}{4\pi G}\nabla \cdot g - \rho_{\rm b}, \tag{6}$$

where $g$ is the MOND gravitational acceleration given by equation (2) and $\rho_{\rm b}$ is the density of detectable baryonic matter. Asymptotically, the MOND acceleration (the solution determined by equation 2 about a point mass) goes as

$$g = \frac{\sqrt{GMa_0}}{r} \tag{7}$$

then equation (6) implies that in the outer regions

$$\rho_{\rm pdm} = \frac{1}{4\pi}\sqrt{\frac{Ma_0}{G}}\frac{1}{r^2} \tag{8}$$

as in an isothermal sphere. Because this phantom halo is seen in projection, it will contribute roughly 15 per cent of the total *projected* mass within an Einstein ring (the exact fraction depends upon the interpolating function $\mu$).

Of course, phantom dark matter is a phantom, but for determining the lensing properties of an object with MOND, the concept is



Downloaded from https://academic.oup.com/mnras/article-abstract/439/2/1781/1013236 by University of Groningen user on 16 November 2018

useful. For example, the MOND critical surface density for strong lensing is identical to that given by equation (3) when the projected phantom dark matter is included; the true surface density of projected baryonic matter is reduced by the same factor (≈15 per cent).

## 3 THE SLACS SAMPLE: LENSING MASSES VERSUS STELLAR MASSES

The SLACS lenses comprise a reasonably large (85), homogeneously selected sample of strong gravitational lenses at redshifts typically between 0.1 and 0.3. Most of the objects are early-type galaxies, elliptical or S0, and a number of these present almost complete Einstein rings, simplifying the modelling and leading to quite unambiguous lensing mass estimates inside the Einstein ring radius. The sloan sky survey observations also include measurements of the stellar velocity dispersions within an aperture of 3 arcsec. Auger et al. (2009) have imaged the lensing galaxies with the *Hubble Space Telescope* in various photometric bands, and the effective radius of the corresponding de Vaucouleurs profile is determined. The broad-band colours permit the fitting of stellar population synthesis models and, thereby, estimates of the stellar mass. An important free function in these models is the form of the IMF, and Auger et al. have considered both the popular Chabrier and Salpeter forms; they tabulate the estimated stellar masses of the lensing galaxies in both cases.

Here I have selected 65 objects from their sample. These are lenses which are classified as elliptical galaxies, and which have complete photometric data, all with estimates of the stellar mass. In the dynamical analysis, I assume that the total light and mass distribution is given by the spherical Jaffe model (Jaffe 1983) with an effective radius appropriate to the particular object. The effective radius is that provided by Auger et al. based upon de Vaucouleurs law fits to the *I*-band photometry; I take this to be representative of the true distribution of starlight and stellar mass (the scalelength of the corresponding Jaffe model is given by $R_{\rm J} = 1.31 R_{\rm eff}$).

Given the numerical value of $F(z_{\rm l}, z_{\rm s})$ (calculated in the context of the standard 'concordance' cosmology which the proper theory of MOND should reproduce) and the effective radius in each case, I adjust the mass of the Jaffe model, for both GR and MOND, in order to match the Einstein ring radius. That is the radius (also given by Auger et al. 2009) within which the enclosed surface density is equal to the critical surface density (equation 3) which, in the case of MOND, includes projected phantom dark matter (equation 6). The projected Jaffe model mass within the Einstein ring radius is the lensing mass for GR or MOND, but with MOND the lensing mass is, on average, 15 per cent lower because of the higher effective gravitational force. I emphasize again that the difference between the GR and MOND lensing mass is equal to the contribution of projected phantom dark matter.

It is the lensing mass in both cases that I will compare with the stellar mass projected within the Einstein ring assuming that the Jaffe model with the *I*-band effective radius describes the luminosity density. One could alternatively choose to compare the total Jaffe mass either for GR or MOND with the total stellar mass, but this obscures the fact that strong lensing provides only a measurement of the projected mass within the Einstein ring.

The observed and derived parameters of the SLACS subsample are given in Table 1. Here for each lens I give (1) the Einstein ring radius in kpc; (2) the *I*-band effective radius in kpc; (3) the total mass of the Jaffe sphere required to produce the observed Einstein ring radius in the context of MOND (in all cases masses are given in units of $10^{11}{\rm M}_{\odot}$); (4) the projected mass within the Einstein ring, the lensing mass, with GR (this is consistent with that given by Auger et al. 2009, table 4, column 3); (5) the projected Jaffe model mass within the Einstein ring in the context of MOND, the MOND lensing mass (the difference between columns 4 and 5 is the contribution of phantom dark matter); (6) the stellar mass (Salpeter) projected within the Einstein ring (this depends upon the effective radius); (7) the fraction of the MOND lensing mass to GR lensing mass; (8) the fraction of projected visible to GR lensing mass (ratio of column 6 to column 4) within the Einstein ring; (9) the total MOND $M/L$ in the visible band. Note that column 3 provides the normalization of the Jaffe model in the context of MOND. The Jaffe mass normalization for GR is obtained by multiplying the MOND Jaffe mass (column 3) by the ratio of the GR lensing mass to the MOND lensing mass (column 4 to column 5).

From the table we see that with MOND there is rather little dispersion of the Jaffe mass fraction within the Einstein radius (column 7): $\langle f_{\rm J}(R_{\rm E})\rangle = 0.855 \pm 0.026$. This is because the Einstein radius depends upon the interior surface density as does the radius of the onset of modified dynamics. With MOND this would be the true baryonic mass in terms of the estimated GR lensing mass. On the other hand, the fraction of stellar mass to GR lensing mass, $f_*(R_{\rm E})$, shows a greater dispersion, with $\langle f_*(R_{\rm E})\rangle = 0.84 \pm 0.19$. The dispersion in this quantity, also given by Auger et al. (2009) (table 4, column 5), reflects the errors, random and systematic, in the population synthesis models for the stellar mass. In general, the results for $f_*(R_{\rm E})$ given here correlate with those of Auger et al. (2009) although their mean value is lower ($\langle f\star\rangle = 0.73 \pm 0.19$) implying a larger fraction of dark matter. This is because of the use of the *I*-band $R_{\rm eff}$ here as opposed to the *V*-band $R_{\rm eff}$ by Auger et al. The effective radii in *V* are generally larger which means a smaller stellar mass projected within the fixed Einstein ring radius. I comment on this in the final section.

The lensing mass with GR (column 4) is plotted against the projected stellar mass (Salpeter) in Fig. 1, and the MOND lensing mass against the projected stellar mass in Fig. 2. As noted above, the MOND lensing mass is lower because of the enhanced deflection due to the larger effective gravitational force. The quantities being plotted here are completely independent: the stellar mass is determined from stellar population models based upon the observed colours of the lenses, and the lensing masses are determined by the Einstein ring radius with the assumed law of gravity.

A quantitative measure of the discrepancy in these objects would be the ratio of the projected to stellar mass. For GR, the mean value of this ratio over the sample is $1.21 \pm 0.27$; with MOND this is $1.03 \pm 0.22$. It is evident that both determinations of the dynamical mass are consistent with each other and with the presence of no discrepancy, as MOND would predict.

When the stellar masses are estimated using the Chabrier IMF, there is an apparent discrepancy with the mean ratio of MOND lensing to stellar mass being $1.90 \pm 0.44$. This demonstrates the importance of the assumed IMF in assertions about the contribution of dark matter within the inner regions of elliptical galaxies: a factor of 2 difference between estimated lensing and stellar masses cannot be taken as evidence for dark matter.

Several of the objects included here (Table 1) have been considered in detail in separate studies. For example, SDSS J1430+4105 was discussed by Eichner, Seitz & Bauer (2012) who argued that several subcomponents in the lensed image constrain on the total mass distribution within the Einstein radius and that the fractional dark mass within the Einstein ring range ranges from 0.2 to 0.4 ($0.6 < f^*(R_{\rm E}) < 0.8$). The lens is complicated by the fact that it is not isolated; there is a surrounding group. Nonetheless, the results

Downloaded from https://academic.oup.com/mnras/article-abstract/439/2/1781/1013236 by University of Groningen user on 16 November 2018

**Table 1.** SLACS sample lenses: observed and derived parameters.

| Lens | (1) $R_{\rm E}$ (kpc) | (2) $R_{\rm eff}$ (kpc) | (3) $M_{\rm J}$(MON) ($10^{11}$ M$_\odot$) | (4) $M_{\rm L}$(GR) ($10^{11}$ M$_\odot$) | (5) $M_{\rm L}$(MON) ($10^{11}$ M$_\odot$) | (6) $M_*(S)(R_{\rm E})$ ($10^{11}$ M$_\odot$) | (7) $f_{\rm J}(R_{\rm E})$ | (8) $f_*(R_{\rm E})$ | (9) $M/L_V$ |
|---|---|---|---|---|---|---|---|---|---|
| 0008−0004 | 6.59 | 9.45 | 6.71 | 3.60 | 2.85 | 1.86 | 0.79 | 0.52 | 5.23 |
| 0029−0055 | 3.48 | 7.63 | 3.02 | 1.22 | 0.99 | 1.26 | 0.81 | 1.03 | 3.13 |
| 0037−0942 | 4.95 | 5.66 | 5.27 | 3.00 | 2.54 | 2.58 | 0.84 | 0.86 | 3.60 |
| 0044+0113 | 1.72 | 4.03 | 2.78 | 0.93 | 0.86 | 0.93 | 0.93 | 1.01 | 3.74 |
| 0157−0056 | 4.89 | 11.10 | 6.80 | 2.68 | 2.21 | 1.78 | 0.83 | 0.67 | 3.80 |
| 0216−0813 | 5.53 | 11.13 | 12.65 | 4.96 | 4.32 | 3.74 | 0.87 | 0.75 | 4.02 |
| 0252+0039 | 4.40 | 5.74 | 4.22 | 1.80 | 1.46 | 1.29 | 0.81 | 0.72 | 4.62 |
| 0330−0020 | 5.45 | 4.38 | 3.66 | 2.57 | 2.07 | 2.14 | 0.81 | 0.83 | 3.09 |
| 0728+3855 | 4.21 | 5.89 | 4.01 | 2.07 | 1.73 | 2.11 | 0.84 | 1.02 | 3.67 |
| 0737+3216 | 4.66 | 8.18 | 6.71 | 3.01 | 2.57 | 3.48 | 0.86 | 1.17 | 3.04 |
| 0819+4534 | 2.73 | 6.20 | 2.92 | 1.11 | 0.96 | 0.81 | 0.86 | 0.73 | 4.03 |
| 0822+2652 | 4.45 | 6.73 | 4.98 | 2.45 | 2.07 | 2.03 | 0.85 | 0.83 | 4.08 |
| 0903+4116 | 7.23 | 9.71 | 8.43 | 4.62 | 3.71 | 3.05 | 0.80 | 0.66 | 3.89 |
| 0912+0029 | 4.58 | 10.97 | 11.69 | 4.08 | 3.62 | 2.85 | 0.89 | 0.70 | 6.35 |
| 0935−0003 | 4.26 | 10.27 | 11.46 | 4.11 | 3.71 | 2.83 | 0.86 | 0.69 | 3.43 |
| 0936+0913 | 3.45 | 6.10 | 3.55 | 1.56 | 1.32 | 1.81 | 0.85 | 1.16 | 3.27 |
| 0946+1006 | 4.95 | 8.17 | 6.32 | 2.96 | 2.49 | 1.53 | 0.84 | 0.52 | 7.06 |
| 0956+5100 | 5.05 | 8.10 | 8.24 | 3.87 | 3.35 | 2.59 | 0.87 | 0.67 | 5.03 |
| 0959+4416 | 3.61 | 7.23 | 4.31 | 1.75 | 1.49 | 1.84 | 0.85 | 1.05 | 3.62 |
| 0959+0410 | 2.24 | 2.83 | 1.49 | 0.78 | 0.68 | 0.64 | 0.87 | 0.82 | 5.35 |
| 1016+3859 | 3.13 | 4.07 | 2.89 | 1.49 | 1.30 | 1.35 | 0.87 | 0.91 | 4.47 |
| 1020+1122 | 5.12 | 6.59 | 6.71 | 3.50 | 3.00 | 2.84 | 0.86 | 0.81 | 4.96 |
| 1023+4230 | 4.50 | 5.48 | 4.36 | 2.44 | 2.05 | 1.73 | 0.84 | 0.71 | 5.29 |
| 1029+0420 | 1.92 | 2.90 | 1.34 | 0.61 | 0.54 | 0.80 | 0.88 | 1.32 | 3.51 |
| 1100+5329 | 7.02 | 9.89 | 9.20 | 4.84 | 3.96 | 2.98 | 0.82 | 0.61 | 4.69 |
| 1103+5322 | 2.78 | 7.56 | 2.87 | 0.98 | 0.82 | 0.99 | 0.84 | 1.02 | 4.12 |
| 1106+5228 | 2.17 | 2.38 | 1.70 | 0.93 | 0.83 | 1.17 | 0.90 | 1.26 | 3.14 |
| 1112+0826 | 6.19 | 5.35 | 7.00 | 4.54 | 3.84 | 2.93 | 0.85 | 0.65 | 5.30 |
| 1134+6027 | 2.93 | 5.23 | 2.97 | 1.29 | 1.12 | 1.22 | 0.87 | 0.94 | 4.58 |
| 1142+1001 | 3.52 | 4.31 | 3.18 | 1.72 | 1.47 | 1.65 | 0.86 | 0.96 | 3.46 |
| 1143−0144 | 3.27 | 5.02 | 4.31 | 2.00 | 1.77 | 1.63 | 0.89 | 0.82 | 3.79 |
| 1153+4612 | 3.18 | 3.08 | 1.85 | 1.15 | 0.96 | 1.11 | 0.84 | 0.97 | 3.65 |
| 1204+0358 | 3.68 | 2.98 | 2.40 | 1.59 | 1.35 | 1.58 | 0.85 | 1.00 | 4.45 |
| 1205+4910 | 4.27 | 6.07 | 5.25 | 2.59 | 2.23 | 2.24 | 0.86 | 0.87 | 4.17 |
| 1213+6708 | 3.13 | 3.22 | 2.55 | 1.49 | 1.30 | 1.56 | 0.87 | 1.05 | 3.04 |
| 1218+0830 | 3.47 | 6.28 | 3.83 | 1.67 | 1.43 | 1.45 | 0.86 | 0.87 | 4.05 |
| 1250+0523 | 4.18 | 4.75 | 3.35 | 1.95 | 1.63 | 1.63 | 0.84 | 0.84 | 2.30 |
| 1306+0600 | 3.87 | 3.57 | 3.55 | 1.77 | 1.54 | 1.36 | 0.87 | 0.77 | 5.37 |
| 1313+4615 | 4.25 | 4.80 | 4.41 | 2.48 | 2.13 | 1.83 | 0.86 | 0.74 | 5.01 |
| 1318−0313 | 6.01 | 9.25 | 6.44 | 3.25 | 2.62 | 1.91 | 0.81 | 0.59 | 4.67 |
| 1330−0148 | 1.32 | 1.43 | 0.65 | 0.34 | 0.31 | 0.23 | 0.90 | 0.68 | 6.42 |
| 1402+6324 | 4.53 | 7.49 | 6.42 | 2.92 | 2.51 | 2.43 | 0.86 | 0.83 | 4.71 |
| 1403+0006 | 2.62 | 3.50 | 1.96 | 1.01 | 0.87 | 1.22 | 0.87 | 1.21 | 3.00 |
| 1416+5136 | 6.08 | 4.23 | 5.16 | 3.72 | 3.08 | 2.54 | 0.83 | 0.68 | 4.87 |
| 1420+6019 | 1.26 | 2.65 | 1.05 | 0.39 | 0.36 | 0.50 | 0.91 | 1.28 | 3.11 |
| 1430+4105 | 6.53 | 10.65 | 11.98 | 5.54 | 4.71 | 3.37 | 0.85 | 0.61 | 6.48 |
| 1436−0000 | 4.80 | 6.81 | 4.48 | 2.34 | 1.92 | 2.09 | 0.82 | 0.90 | 3.01 |
| 1443+0304 | 1.93 | 1.62 | 0.98 | 0.61 | 0.54 | 0.73 | 0.89 | 1.19 | 3.10 |
| 1451−0329 | 2.33 | 3.55 | 1.77 | 0.85 | 0.74 | 1.04 | 0.87 | 1.22 | 2.59 |
| 1525+3327 | 6.55 | 11.79 | 11.12 | 4.91 | 4.10 | 3.90 | 0.83 | 0.79 | 4.08 |
| 1531−0105 | 4.71 | 5.28 | 4.85 | 2.79 | 2.37 | 2.07 | 0.85 | 0.74 | 3.67 |
| 1538+5817 | 2.50 | 2.44 | 1.55 | 0.93 | 0.81 | 0.99 | 0.87 | 1.06 | 3.56 |
| 1614+4522 | 2.54 | 7.54 | 2.34 | 0.74 | 0.61 | 0.79 | 0.83 | 1.07 | 3.54 |
| 1621+3931 | 4.97 | 5.65 | 5.35 | 3.03 | 2.57 | 2.41 | 0.85 | 0.80 | 3.77 |
| 1627−0053 | 4.18 | 6.44 | 4.94 | 2.35 | 2.01 | 2.03 | 0.85 | 0.86 | 4.79 |
| 1630+4520 | 6.91 | 6.23 | 7.63 | 4.93 | 4.09 | 3.88 | 0.83 | 0.79 | 5.40 |
| 1636+4707 | 3.96 | 5.96 | 3.64 | 1.79 | 1.50 | 1.77 | 0.84 | 0.99 | 3.67 |
| 1644+2625 | 3.07 | 3.65 | 2.49 | 1.35 | 1.17 | 1.26 | 0.87 | 0.93 | 3.99 |
| 1719+2939 | 3.89 | 4.33 | 3.45 | 1.98 | 1.69 | 1.40 | 0.86 | 0.71 | 5.22 |

Downloaded from https://academic.oup.com/mnras/article-abstract/439/2/1781/1013236 by University of Groningen user on 16 November 2018

**Table 1** – *continued*

| Lens | (1) $R_E$ (kpc) | (2) $R_{eff}$ (kpc) | (3) $M_J$(MON) ($10^{11}$ $M_\odot$) | (4) $M_L$(GR) ($10^{11}$ $M_\odot$) | (5) $M_* L$(MON) ($10^{11}$ $M_\odot$) | (6) $M^*(S)(R_E)$ ($10^{11}$ $M_\odot$) | (7) $f_J(R_E)$ | (8) $f_*(R_E)$ | (9) $M/L_V$ |
|---|---|---|---|---|---|---|---|---|---|
| 2238−0754 | 3.08 | 4.29 | 2.61 | 1.31 | 1.13 | 1.22 | 0.86 | 0.93 | 3.80 |
| 2300+0022 | 4.51 | 5.39 | 5.62 | 3.04 | 2.64 | 2.09 | 0.87 | 0.69 | 5.88 |
| 2303+1422 | 4.35 | 7.68 | 6.23 | 2.70 | 2.32 | 1.94 | 0.86 | 0.72 | 4.87 |
| 2321−0939 | 2.47 | 6.17 | 3.68 | 1.23 | 1.10 | 1.21 | 0.89 | 0.98 | 4.14 |
| 2341+0000 | 4.50 | 7.15 | 4.84 | 2.32 | 1.94 | 2.16 | 0.93 | 0.89 | 4.00 |
| 2347−0005 | 6.10 | 6.11 | 7.93 | 4.76 | 4.06 | 3.46 | 0.86 | 0.73 | 3.69 |

(1) The Einstein ring radius in kpc; (2) *I*-band effective radius in kpc; (3) total Jaffe model mass with modified dynamics or relativistic equivalent such as TeVeS; (4) projected GR lensing mass within the Einstein ring; (5) projected MOND lensing mass within the Einstein ring; (6) the projected stellar mass (Salpeter) within the Einstein ring; (7) the projected fraction of the MOND model mass within the Einstein ring radius with MOND (the remainder being phantom dark matter); (8) the projected fraction of stellar mass within the Einstein ring, the remainder being Jaffe plus phantom dark matter (with MOND); (9) MOND $M/L_V$.

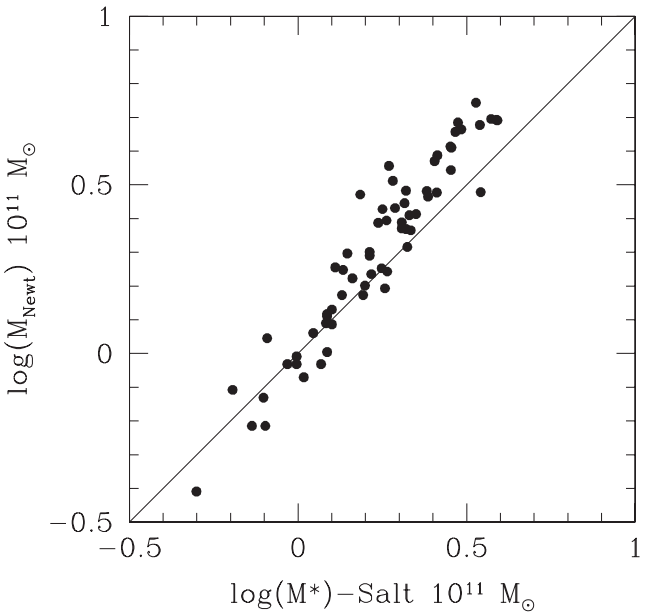


**Figure 1.** The logarithm of the GR lensing mass of SLACS lenses plotted against that of the stellar mass projected within the Einstein ring assuming the Salpeter IMF (given by Auger et al. 2009). Both are given in units of $10^{11}$ $M_\odot$ and the equality line is shown.

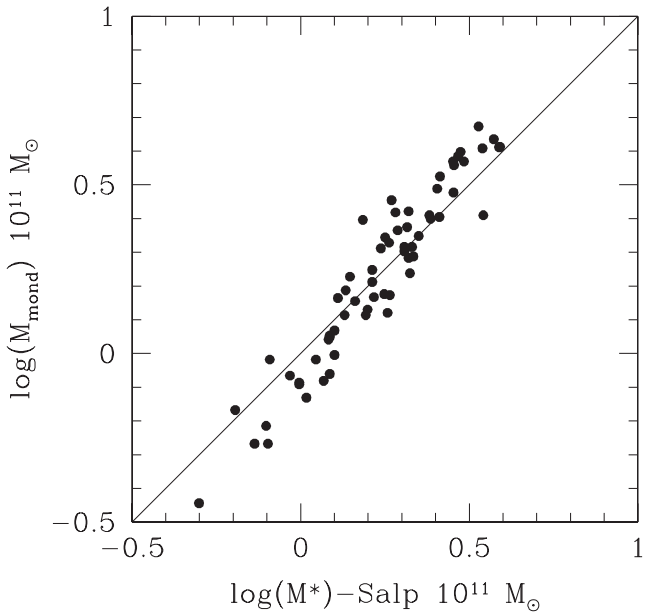


**Figure 2.** As in Fig. 1 but here the logarithm of the MOND lensing mass is plotted against the stellar mass (Salpeter) projected within the Einstein ring.

are roughly consistent with those given here with $f^* = 0.61$. The total $M/L_V$ of this object (with modified dynamics) is the second largest of the sample (6.48), but it is certainly not an outlier from the distribution of points in Fig. 2.

We see from Figs 1 and 2 that there is some evidence for a larger discrepancy at larger galaxy stellar masses (the points appear to form a steeper relation than the equality line). Indeed, there are claims that the IMF systematically varies with galaxy mass or velocity dispersion towards being more bottom heavy, i.e. there is a larger stellar $M/L$ in more massive systems (Spiniello et al. 2013). There is support for this claim in Fig. 3: here the MOND lensing $M/L$s are plotted against the observed stellar velocity dispersions. The horizontal line represents the mean $M/L_V$ in the rest frame of $4.2 \pm 1.0$. The points with error bars are the $M/L$ averaged in bins of 15 objects and the line is the relation suggested by Spiniello et al. on the basis of spectroscopic tracers of low-mass stars. We see that the distribution of MOND lensing $M/L$s is reasonable for elliptical galaxy stellar populations and that there is marginal evidence for an increase in $M/L$ with velocity dispersion.

## 4 ASSESSMENT

Statements about the need for non-baryonic dark matter within the bright visible inner regions of strong gravitational lenses – early-type galaxies – are not supported by the evidence given here. Figs 1 and 2 demonstrate that the GR and MOND lensing masses are consistent with each other and with the masses of the stellar components determined from population synthesis modelling using the Salpeter IMF. This is in agreement with the expectation from MOND: there should be little discrepancy between the visible and the Newtonian lensing mass within high surface brightness early-type systems; the discrepancies only appear in the outer regions. It is also evident that the uncertainties introduced by the assumed IMF are at least a factor of 2. Within this factor, no assertion about the need for dark matter based upon use of a particular stellar IMF can be credible.

These conclusions are quite independent of the way in which the systems are modelled. Use of Hernquist (1990) rather than Jaffe models gives similar results but with slightly higher ratios of lensing mass to stellar mass (about 6 per cent on average). The Hernquist model does have the advantage that in a given object the radial distribution of stellar velocity dispersion is more nearly constant (isothermal) as observed. Since the two classes of models bracket



Downloaded from https://academic.oup.com/mnras/article-abstract/439/2/1781/1013236 by University of Groningen user on 16 November 2018

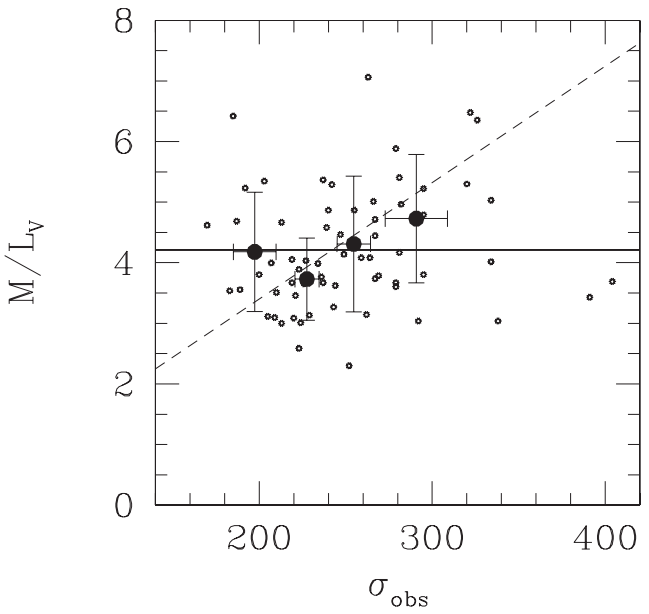


**Figure 3.** The MOND $M/L$s (visual band) of the SLAC lenses in the rest frame plotted against the observed central velocity dispersions. The solid horizontal line shows the average $M/L$ ($4.2 \pm 1.0$), and the large points with error bars denote the mean $M/L$s averaged in bins of 15 objects. The dashed line shows the fit to stellar $M/L$ as a function of velocity dispersion given by Spiniello et al. (2013).

the empirical de Vaucouleurs law (Sand et al. 2004), for which the effective radius is measured, the use of an exact $r^{1/4}$ model would certainly lie within this range of 6 per cent.

It is interesting that Auger et al. (2010) claim that these observations do imply the existence of dark matter within the inner parts of ellipticals. There are two reasons for the difference with the conclusions of the present work. The first is that for Auger et al. the bench mark for defining the inner regions is one-half the effective radius, whereas here I take the Einstein ring radius. With respect to MOND, this is more appropriate because the onset of modified dynamics (or the appearance of 'dark matter') is tied to the enclosed surface density as is the location of the Einstein ring. Secondly, Auger et al. use the $V$-band effective radius, whereas here the $I$-band effective radius is taken as the indicator of the distribution of light and stellar mass. Whichever is more appropriate, the differences in the estimated stellar mass within the Einstein ring are not large and within the uncertainties of population synthesis modelling.

Most of the claims of need for dark matter within the Einstein radius are based upon observations of more distant systems, such as those of the CASTLES sample (Ferreras et al. 2012). These lenses have a wide distribution of redshifts, with typically $z_l \approx 0.4$–$0.5$ but ranging up to $z_l \approx 1$. These are generally more complicated lens systems with multiple images and relatively few complete Einstein rings; therefore, the lens modelling is less certain. Moreover, for these distant lenses it is more difficult to detect contamination by background objects – groups or clusters surrounding the lens or along the line of sight – and it does appear that the contamination rate is higher for this sample (Leier et al. 2011). It would seem to require substantial structural evolution since $z = 1$ if the lenses in this sample really do have more dark matter in the inner regions than the objects in the relatively nearby homogeneous and clean SLACS sample.

Overall, the MOND prediction of no significant discrepancy between the Newtonian dynamical mass and stellar mass within the inner high surface brightness regions is supported by this analysis of the SLACS sample. Indeed, one can turn the argument around: Figs 1 and 2 support the validity of stellar population synthesis models in determining the mass of the stellar component.

## ACKNOWLEDGEMENTS

I thank Leon Koopmans, Chiara Spiniello, Moti Milgrom, Stacy McGaugh and Marcel Pawlowsky for helpful comments. An anonymous referee suggested numerous improvements in the presentation of these results.

## REFERENCES

Auger M. W., Treu T., Bolton A. S., Gavazzi R., Koopmans L. V. E., Marshall P. J., Bundy K., Moustakas L. A., 2009, ApJ, 705, 1099
Auger M. W., Treu T., Bolton A. S., Gavazzi R., Koopmans L. V. E., Marshall P. J., Bundy K., Moustakas L. A., 2010, ApJ, 724, 511
Bekenstein J. D., 2004, Phys. Rev. D, 70, 03509
Chabrier G., 2003, PASP, 115, 763
Chen D. M., Zhao H.-S., 2006, ApJ, 650, L9
Chiu M.-C., Ko C-M., Tian Y., 2006, ApJ, 636, 565
Chiu M.-C., Ko C.-M., Tian Y., Zhao H.-S., 2011, Phys. Rev. D, 83, 063583
Conroy C., van Dokkum P., 2012, ApJ, 747, 69
Conroy C., Dutton A. A., Graves G. J., Mendel J. T., van Dokkum P. G., 2013, ApJ, 776, L26
Eichner T., Seitz S., Bauer A., 2012, MNRAS, 427, 1918
Famaey B., McGaugh S., 2012, Living Rev. Relativ., 15, 10
Ferreras I., Mavromatos N. E., Sakellariadou M., Yusaf M. F., 2009, Phys. Rev. D, 80, 103506
Ferreras I., Mavromatos N. E., Sakellarieadou M., Yusaf M. F., 2012, Phys. Rev. D, 86, 3507
Hernquist L., 1990, ApJ, 356, 359
Jaffe W., 1983, MNRAS, 202, 995
Leier D., Ferreras I., Saha P., Falco E., 2011, ApJ, 740, 97
Mavromatos N. E., Sakellariadou M., Yusaf M. F., 2009, Phys. Rev. D, 79, 1301
McGaugh S. S., 2005, ApJ, 632, 859
Milgrom M., 1983, ApJ, 270, 371
Milgrom M., 2012, Phys. Rev. Lett., 109, 131101
Milgrom M., 2013, Phys. Rev. Lett., 111, 041105
Milgrom M., Sanders R. H., 2003, ApJ, 599, L25
Romanowsky A. J., Douglas N. G., Arnaboldi M., Kuijken K., Merrifield M. R., Napolitano N. R., Capaccioli M., Freeman K. C., 2003, Science, 301, 1696
Salpeter E. E., 1955, ApJ, 121, 161
Sand D. J., Treu T., Smith G. P., Ellis R. S., 2004, ApJ, 604, 88
Sanders R. H., Land D. D., 2008, MNRAS, 389, 701
Sanders R. H., Noordermeer E., 2007, MNRAS, 379, 702
Smith R. J., Lucey J. R., Carter D., 2012, MNRAS, 426, 2994
Spiniello C., Trager S. C., Koopmans L. V. E., Chen Y. P., 2012, ApJ, 753, L32
Spiniello C., Trager S. C., Koopmans L. V. E., Conroy C., 2013, MNRAS, preprint (arXiv:1305.2873)
Swaters R. A., Sanders R. H., McGaugh S. S., 2010, ApJ, 718, 380
Trachternach C., de Blok W. J. G., Walter F., Brinks E., Kennicutt R. C., Jr, 2008, AJ, 136, 2720
Zhao H.-S., Famaey B., 2006, ApJ, 638, L9

This paper has been typeset from a TEX/LATEX file prepared by the author.



Downloaded from https://academic.oup.com/mnras/article-abstract/439/2/1781/1013236 by University of Groningen user on 16 November 2018